arXiv:1205.5667v1 [quant-ph] 25 May 2012

Study of maximal bipartite entanglement in valence-bond states

Muzaffar Q. Lone[1] and Sudhakar Yarlagadda[1,2]
[1]*TCMP Div.* and [2]*CAMCS*
1/AF Salt Lake, Saha Institute of Nuclear physics,
Kolkata, India -700064

(Dated: March 4, 2013)

We study maximal bipartite entanglement in valence-bond (VB) states and show that the average bipartite entanglement E_v^2, between a sub-system of two spins and the rest of the system, can be maximized through a homogenized superposition of the VB states. Our derived maximal E_v^2 rapidly increases with system size and saturates at its maximum allowed value. We adopt two ways of generating maximal E_v^2 states: (i) starting with a general superposition of VB states, we impose homogeneity; (ii) by considering a general homogeneous state, we generate isotropy. By using these two approaches, we construct explicitly four-qubit and six-qubit highly entangled states that are both isotropic and homogeneous. We also demonstrate that our maximal E_v^2 states are ground states of an isotropic infinite range Heisenberg model (IIRHM) and represent a new class of resonating-valence-bond (RVB) states.

PACS numbers: 03.67.Mn, 03.65.Ud, 03.67.Bg, 75.10.Jm

I. INTRODUCTION

Quantum entanglement, a manifestation of non-locality, is a precious resource for quantum computation and quantum information [1] and signifies correlations in many-body systems. Quantum algorithms that would significantly accelerate a classical computation must rely on highly entangled states since slightly entangled states can be simulated efficiently on a classical computer [2]. The strength of correlations of fluctuations of observables (such as density, magnetization, etc.) in a many-body system is a reflection of the degree of entanglement (for pure states) [3]. Thus, characterization of multi-particle entanglement and production of maximal/high multi-qubit entanglement is vital for quantum computational studies and for mutual enrichment of quantum information and many-body condensed matter physics.

Intensive work on entanglement during the past decade has led to the proposal of numerous measures of entanglement [4, 5]. While two-party entanglement is quite well understood, entanglement in a multi-party system is an area of immense current interest [6–13]. In the quest for maximally entangled states, so far only few-qubit maximally entangled states such as two-qubit Bell states, three-qubit Greenberger-Horne-Zeilinger (GHZ) states, and four-qubit Higuchi-Sudbery (HS) states [14] have been clearly identified. It would be of considerable interest to generate these maximally entangled states as the ground states of a physically realizable spin model. While the GHZ states could be obtained as the ground state of an anisotropic Heisenberg model [15] maximally entangled four-qubit and five-qubit states could be obtained only as excited states [16].

VB states are useful in understanding the entanglement properties of cluster states that enable universal quantum computation [17, 18]. Furthermore, VB states are also useful as variational states with valence bond length being the variational degree of freedom [19–21]. RVB states are the linear superpositions of VB states and have provided interesting insights for understanding strongly correlated phenomena such as spin liquid physics in frustrated magnets [22], physics of high T_c cuprates [23–25], superconductivity in organic solids [26], insulator-superconductor transition in boron-doped diamond [27], etc. Furthermore, RVB states have also been proposed as robust basis states for topological quantum computation [28]. The multi-particle entanglement has also been investigated in RVB states that were proposed as states close in energy to the ground state of the Heisenberg Hamiltonian [29–31]. However, there has been no explicit construction of RVB states that would represent maximally entangled VB states.

The main results of this paper are threefold. First, we study the entanglement defined by von Neumann entropy and show that isotropy and homogeneity maximize the bipartite entanglement E_v^2. Second, based on these principles of isotropy and homogeneity, we propose two approaches to construct entangled states that maximize E_v^2. Lastly, we analyze these states in terms of ground states of IIRHM and observe that these states represent a new class of RVB states.

The remainder of this paper is organized as follows. In section II, we introduce entanglement entropy and demonstrate explicitly that isotropy and homogeneity maximize entanglement E_v^2 between two spins and the rest of the system in the two limits of even-N-qubits, i.e., for $N = 4$ and $N \to \infty$. For intermediate even-N-spin states, our proposed entangled states are only shown to maximize E_v^2 among VB states. In section III, we provide two approaches to construct maximal E_v^2 entangled states: first approach deals with homogenizing isotropic states while the second one generates isotropy in homogeneous states. We also demonstrate our procedures by constructing maximal E_v^2 states for four-qubit and six-qubit systems. In section IV, we show that our $E_{v,max}^2$ states are ground states of our IIRHM while in section V, we make a comparison of our $E^2_{v,max}$ states with the RVB states and observe that our maximal E^2_v states represent a new class of RVB states. Lastly, in the final section VI, we conclude after commenting on the physical realizability and decoherence free nature of our proposed high E^2_v entangled states.

II. ENTANGLEMENT FOR TWO-QUBIT REDUCED DENSITY MATRIX IN ISOTROPIC SYSTEM.

For a bipartite system AB in a pure state, von Neumann entropy E_v measures the entanglement between the subsystems A and B. From the reduced density matrices $\rho_A \equiv tr_B \rho^{AB}$ and $\rho_B \equiv tr_A \rho^{AB}$ obtained from the pure state ρ^{AB}, we obtain

$$\begin{aligned} E_v(\rho_A) &= -tr(\rho_A \log_2 \rho_A) \\ &= -tr(\rho_B \log_2 \rho_B) = E_v(\rho_B). \end{aligned} \tag{1}$$

Using the basis $|\downarrow\rangle$, $|\uparrow\rangle$, and $S^i = \frac{1}{2}\sigma^i$, the single qubit density matrix can be written as [33]

$$\rho_i = \begin{bmatrix} \frac{1}{2} - \langle S^z_i \rangle & \langle S^+_i \rangle \\ \langle S^-_i \rangle & \frac{1}{2} + \langle S^z_i \rangle \end{bmatrix}. \tag{2}$$

Throughout this paper, we consider only states $|\Psi\rangle$ that are eigenstates of the z-component of the total spin operator (S^z_{Total}) with eigenvalue S^z_T; furthermore, we focus on only isotropic states. It then follows that, $\langle S^z_i \rangle = 0$ and $\langle S^+_i \rangle = 0$ leading to the single-qubit density matrix to be maximally mixed and thus maximizing entanglement $E_v(\rho_i)$. On realizing that $\langle S^z_i \rangle = 0$, we obtain the following expression for the two-qubit reduced density matrix [33]:

$$\rho_{ij} = \begin{bmatrix} \frac{1}{4} + \langle S^z_i S^z_j \rangle & 0 & 0 & 0 \\ 0 & \frac{1}{4} - \langle S^z_i S^z_j \rangle & \langle S^+_i S^-_j \rangle & 0 \\ 0 & \langle S^-_i S^+_j \rangle & \frac{1}{4} - \langle S^z_i S^z_j \rangle & 0 \\ 0 & 0 & 0 & \frac{1}{4} + \langle S^z_i S^z_j \rangle \\ . & & & \end{bmatrix}. \tag{3}$$

Here, isotropy implies $0.5\langle S^-_i S^+_j \rangle = 0.5\langle S^+_i S^-_j \rangle = \langle S^x_i S^x_j \rangle = \langle S^y_i S^y_j \rangle = \langle S^z_i S^z_j \rangle$. Thus, the von Neumann entropy $E_v(\rho_{ij})$ can be expressed as

$$\begin{aligned} E_v(\rho_{ij}) = 2 - \frac{1}{4} \ [\ & 3(1 + 4\langle S^z_i S^z_j \rangle) \log_2(1 + 4\langle S^z_i S^z_j \rangle) \\ & + \ (1 - 12\langle S^z_i S^z_j \rangle) \log_2(1 - 12\langle S^z_i S^z_j \rangle)] \end{aligned} \tag{4}$$

For our states, $S^z_{Total}|\Psi\rangle = 0$ which implies that $\langle S^z_i \sum_j S^z_j \rangle = 0$, that is,

$$\sum_{j \neq i} \langle S^z_i S^z_j \rangle = -\langle {S^z_i}^2 \rangle = -\frac{1}{4}. \tag{5}$$

We will now maximize the total entanglement entropy $\sum_{i,j\neq i} E_v(\rho_{ij})$ subject to the above constraint in Eq. (5). To this end, we will employ the method of Lagrange multipliers and define the Lagrange function Λ as follows:

$$\Lambda = \sum_{i,j\neq i} E_v(\rho_{ij}) - \sum_i \lambda_i \left(\sum_{j \neq i} \langle S^z_i S^z_j \rangle + \frac{1}{4} \right). \tag{6}$$

Then, setting $\frac{\partial \Lambda}{\partial \langle S^z_l S^z_m \rangle} = 0$ yields

$$\lambda_l = 3 \log_2 \left[\frac{(1 - 12\langle S^z_l S^z_m \rangle)}{(1 + 4\langle S^z_l S^z_m \rangle)} \right], \tag{7}$$

which implies that the optimal $\langle S^z_i S^z_j \rangle$ is independent of j for $j \neq i$. Consequently, it follows from Eq. (5) that $\sum_{i,j\neq i} E_v(\rho_{ij})$ is maximized when $\langle S^z_i S^z_j \rangle = -\frac{1}{4(N-1)}$, i.e., when the isotropic state is *homogeneous*. The average entanglement entropy between the subsystem of two spins and the rest of the system (of $N-2$ spins) $E^2_v \equiv [1/N(N-1)] \sum_{i,j\neq i} E_v(\rho_{ij})$ has a maximum value given by

$$\begin{aligned} E^2_{v,max} \ = \ & -3 \left(\frac{1}{4} - \frac{1}{4(N-1)} \right) \log_2 \left(\frac{1}{4} - \frac{1}{4(N-1)} \right) \\ & - \ \left(\frac{1}{4} + \frac{3}{4(N-1)} \right) \log_2 \left(\frac{1}{4} + \frac{3}{4(N-1)} \right). \end{aligned} \tag{8}$$

It is interesting to note that for $N \to \infty$, the above expression yields $E^2_v \to 2$. In fact, E^2_v approaches the maximum possible value 2 quite rapidly as can be seen from Fig. 1. Next, we observe that for $N = 4$, our expression for $E^2_{v,max}$ in Eq. (8) yields the same entanglement entropy value $1 + 0.5 \log_2 3$ as that obtained for the four-qubit maximally entangled HS state [10, 14]. Furthermore, our approach explains why all the pairs in the HS state give the same entanglement value. Contrastingly, for the isotropic ground state, in the case of a Heisenberg chain with nearest-neighbor interaction, for four spins the entanglement entropy $E^2_v = 1.21$ (with $\langle S^z_i S^z_j \rangle = -0.5/3$) while for an infinite chain the von Neumann entropy $E^2_v = 1.37$ (with $\langle S^z_i S^z_j \rangle \approx -0.443/3$) both of which are far less than our maximal E^2_v values above. It is of interest to note that, when $N = 4$ or $N \to \infty$, the maximal values of E^2_v for isotropic systems are the same as the maximal E^2_v values for general systems (i.e., systems that can be either isotropic or non-isotropic).

We also note that homogeneity, under the constraint of Eq. (5), maximizes the i-concurrence (I_c) [34] given by

$$I_c = \frac{2}{N(N-1)} \sum_{i,j>i} \sqrt{2[1 - Tr(\rho^2_{ij})]}. \tag{9}$$

As shown in Fig. 1, I_c also monotonically increases with system size. Although we considered von Neumann entropy and i-concurrence as entanglement measures, our homogeneous states should also maximize other measures of entanglement for ρ_{ij} in VB systems.

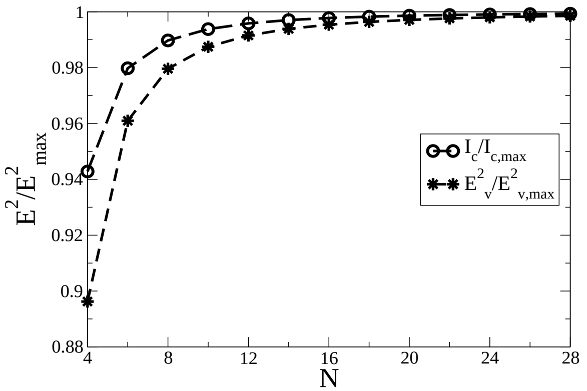

FIG. 1: Normalized entanglement $E^2/E^2_{\max}$, for two-qubit reduced density matrix, measured by (a) von Neumann entropy ($E^2_v/E^2_{v,\max}$) and (b) i-concurrence ($I_c/I_{c,\max}$), for N-qubit VB systems.

III. MAXIMAL E_v^2 ENTANGLED STATES

In this section we offer two different approaches for constructing maximal E_v^2 states; the first approach involves producing homogeneity in isotropic states while the second deals with generating isotropy in homogeneous states. As examples of our prescribed procedure, we construct highly entangled states for four and six qubits.

A. Generating homogeneity in isotropic states

In this section we will proceed to construct entangled states for N-spins that maximize E_v^2. We first note that there are $(N-1)!!$ states with $S_T = 0$ which are the product of $N/2$ two-spin singlet states of the form $|\uparrow\downarrow\rangle - |\downarrow\uparrow\rangle$ (with no pair of singlets sharing a spin). Of these $(N-1)!!$ product combinations with $S_T = 0$, only ${}^N C_{\frac{N}{2}} - {}^N C_{\frac{N}{2}-1} = N!/[(N/2)!(N/2+1)!]$ products are linearly independent. A particular set of linearly independent $S_T = 0$ states are the Rumer states [35, 36] that are made up of non-crossing singlets.

Next, we demonstrate how highly entangled states can be constructed by starting from isotropic states and making them homogeneous. Since we are dealing with spin-singlets, we consider $\frac{N}{2}\uparrow$ spins and $\frac{N}{2}\downarrow$ spins in our basis states $|\psi_k^z\rangle$ ($\equiv |\sigma_1^z\sigma_2^z...\sigma_N^z\rangle$ where $\sigma_i^z =\uparrow$ or $\downarrow$). Using superposition of these basis states, with all states having equal probability, we construct the states

$$|\Psi_N\rangle_{hom} = \sum_{k=1}^{{}^N C_{N/2}} e^{i\delta_k}|\psi_k^z\rangle, \qquad (10)$$

which we will now prove to be homogeneous. Throughout this paper, for convenience, we ignore the normalization constants in our spin states. Let the spin at site i be either $\uparrow$ or $\downarrow$; then the probability that the spin at site $j \neq i$ is in the same state is $\frac{[(N/2)-1]}{[(N/2)-1]+N/2}$ while the probability that it is in the opposite state is $\frac{[N/2]}{[(N/2)-1]+N/2}$. Therefore, we can write

$$\begin{aligned}\langle S_i^z S_j^z\rangle &= \frac{1}{4}\left[\frac{\frac{N}{2}-1}{(\frac{N}{2}-1)+\frac{N}{2}}\right] - \frac{1}{4}\left[\frac{\frac{N}{2}}{(\frac{N}{2}-1)+\frac{N}{2}}\right] \\ &= -\frac{1}{4(N-1)}. \qquad (11)\end{aligned}$$

Thus, when all the basis states are equally probable, we get $\langle S_i^z S_j^z\rangle = -\frac{1}{4(N-1)}$. Now, we are in a position to form (from isotropic $S_T = 0$ states) homogenized states that are highly entangled.

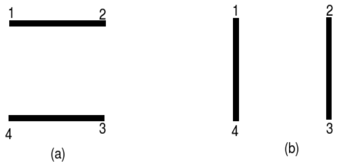

FIG. 2: Linearly independent non-crossing Rumer diagrams for a four qubit system .

Four Qubit maximal E_v^2 states: For $N = 4$ spins, we have two linearly independent non-crossing Rumer diagrams which are shown in Fig. 2. The states corresponding to these diagrams can be expressed as $|\Phi_{12}^{S_{12}=0}\rangle \otimes |\Phi_{34}^{S_{34}=0}\rangle$ and $|\Phi_{14}^{S_{14}=0}\rangle \otimes |\Phi_{23}^{S_{23}=0}\rangle$ where $|\Phi_{ij}^{S_{ij}=0}\rangle \equiv [|\uparrow\rangle_i|\downarrow\rangle_j - |\downarrow\rangle_i|\uparrow\rangle_j]$ is a two-spin singlet state for spins at sites i and j with S_{ij} being the total spin of S_i and S_j. It is worth noting that

$$\begin{aligned}|\Phi_{13}^{S_{13}=0}\rangle \otimes |\Phi_{24}^{S_{24}=0}\rangle &= |\Phi_{12}^{S_{12}=0}\rangle \otimes |\Phi_{34}^{S_{34}=0}\rangle \\ &\quad + |\Phi_{14}^{S_{14}=0}\rangle \otimes |\Phi_{23}^{S_{23}=0}\rangle. \qquad (12)\end{aligned}$$

This means that the crossing singlet $|\Phi_{13}^{S_{13}=0}\rangle \otimes |\Phi_{24}^{S_{24}=0}\rangle$ depends linearly on the two non-crossing singlets $|\Phi_{12}^{S_{12}=0}\rangle \otimes |\Phi_{34}^{S_{34}=0}\rangle$ and $|\Phi_{14}^{S_{14}=0}\rangle \otimes |\Phi_{23}^{S_{23}=0}\rangle$. Using the above relation one can establish that there are only ${}^N C_{\frac{N}{2}} - {}^N C_{\frac{N}{2}-1}$ linearly independent $S_T = 0$ states.

Next, we take the following linear superposition that will lead us to the desired entangled state:

$$\begin{aligned}|\Psi^4\rangle &= r_1 e^{i\theta_1}\left[|\Phi_{12}^{S_{12}=0}\rangle \otimes |\Phi_{34}^{S_{34}=0}\rangle\right] \\ &+ r_2 e^{i\theta_2}\left[|\Phi_{14}^{S_{14}=0}\rangle \otimes |\Phi_{23}^{S_{23}=0}\rangle\right], \qquad (13)\end{aligned}$$

where $r_i e^{i\theta_i}$ represents a general coefficient.

Evaluating Eq. (13) (and setting $|\Psi^4\rangle = |\Psi_N\rangle_{hom}$ for $N = 4$), we get the various coefficients (shown in Table I) for each of the basis state $|\psi_k^z\rangle$ occurring in Eq. (10).

The expression for $|\Psi^4\rangle$ [in Eq. (13)] assumes the homogenized superposed form shown in Eq. (10) for two linearly independent sets of solutions of the coefficients in Table I; the two sets of solutions are $\{r_1 e^{i\theta_1} =$

Basis states $\|\psi_k^z\rangle$	Coefficients $e^{i\delta_k}$ in Eq. (10).
$\|\uparrow\downarrow\uparrow\downarrow\rangle$	$r_1e^{i\theta_1} - r_2e^{i\theta_2}$
$\|\downarrow\uparrow\downarrow\uparrow\rangle$	$r_1e^{i\theta_1} - r_2e^{i\theta_2}$
$\|\uparrow\downarrow\downarrow\uparrow\rangle$	$-r_1e^{i\theta_1}$
$\|\downarrow\uparrow\uparrow\downarrow\rangle$	$-r_1e^{i\theta_1}$
$\|\uparrow\uparrow\downarrow\downarrow\rangle$	$r_2e^{i\theta_2}$
$\|\downarrow\downarrow\uparrow\uparrow\rangle$	$r_2e^{i\theta_2}$

TABLE I: Basis states $|\psi_k^z\rangle$ of Eq. (10) for a four-qubit system and the corresponding coefficients $e^{i\delta_k}$ obtained by setting $|\Psi^4\rangle$ [in Eq. (13)] equal to $|\Psi_N\rangle_{hom}$ [in Eq. (10)] with $N = 4$.

$e^{i2\pi/3}, r_2e^{i\theta_2} = e^{i4\pi/3}\}$ and its complex conjugate. The states corresponding to these solutions are

$$\begin{aligned}
|\Psi^4\rangle &= e^{i2\pi/3}(|\Phi_{12}^{S_{12}=0}\rangle \otimes |\Phi_{34}^{S_{34}=0}\rangle) \\
&+ e^{i4\pi/3}(|\Phi_{14}^{S_{14}=0}\rangle \otimes |\Phi_{23}^{S_{23}=0}\rangle) \\
&= [(|\uparrow\downarrow\uparrow\downarrow\rangle + |\downarrow\uparrow\downarrow\uparrow\rangle) + \omega_3(|\uparrow\downarrow\downarrow\uparrow\rangle + |\downarrow\uparrow\uparrow\downarrow\rangle) \\
&\qquad + \omega_3^2\ (|\uparrow\uparrow\downarrow\downarrow\rangle + |\downarrow\downarrow\uparrow\uparrow\rangle)] \\
&\equiv |\Psi_{\mathrm{HS}}\rangle \qquad (14)
\end{aligned}$$

and its complex conjugate. In the above equation, $\omega_3 = e^{i2\pi/3}$, i.e., a cube root of unity. The above state is the well known Higuchi-Sudbery (HS) state for four qubits [14].

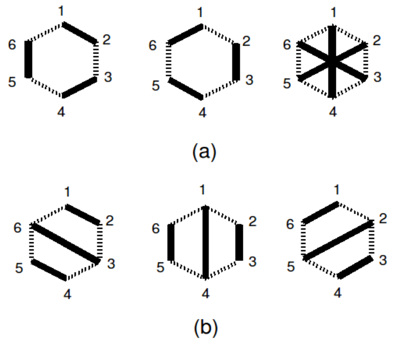

FIG. 3: Homogenized linear combination of the five non-crossing $S_T = 0$ singlet states (or non-crossing Rumer diagrams) in (a) and (b) give maximal E_v^2 entanglement for six qubits. The state $|\Psi_c^6\rangle$ in Eq. (19) is a linear combination of the three diagrams in (a); on the other hand, $|\Psi_a^6\rangle$ and $|\Psi_b^6\rangle$ in Eqs. (16) and (17), respectively, represent different linear combinations of all the three diagrams in (b).

Basis states ψ_k^z	Coefficients $e^{i\delta_k}$ in Eq. (10).
$\|\uparrow\downarrow\uparrow\downarrow\uparrow\downarrow\rangle$	$r_1e^{i\theta_1}$ $-r_2e^{i\theta_2}$ $-r_3e^{i\theta_3}$ $-r_4e^{i\theta_4}$ $-r_5e^{i\theta_5}$
$\|\downarrow\uparrow\uparrow\downarrow\uparrow\downarrow\rangle$	$-r_1e^{i\theta_1}$ $+r_3e^{i\theta_3}$
$\|\uparrow\downarrow\downarrow\uparrow\uparrow\downarrow\rangle$	$-r_1e^{i\theta_1}$ $+r_5e^{i\theta_5}$
$\|\downarrow\uparrow\downarrow\uparrow\uparrow\downarrow\rangle$	$r_1e^{i\theta_1}$ $-r_4e^{i\theta_4}$
$\|\uparrow\downarrow\uparrow\downarrow\downarrow\uparrow\rangle$	$-r_1e^{i\theta_1}$ $+r_4e^{i\theta_4}$
$\|\downarrow\uparrow\uparrow\downarrow\downarrow\uparrow\rangle$	$r_1e^{i\theta_1}$ $-r_5e^{i\theta_5}$
$\|\uparrow\downarrow\downarrow\uparrow\downarrow\uparrow\rangle$	$r_1e^{i\theta_1}$ $-r_3e^{i\theta_3}$
$\|\downarrow\uparrow\downarrow\uparrow\downarrow\uparrow\rangle$	$-r_1e^{i\theta_1}$ $+r_2e^{i\theta_2}$ $+r_3e^{i\theta_3}$ $+r_4e^{i\theta_4}$ $+r_5e^{i\theta_5}$
$\|\uparrow\uparrow\downarrow\downarrow\uparrow\downarrow\rangle$	$+r_2e^{i\theta_2}$ $+r_4e^{i\theta_4}$
$\|\uparrow\uparrow\downarrow\downarrow\downarrow\uparrow\rangle$	$-r_4e^{i\theta_4}$
$\|\downarrow\downarrow\uparrow\uparrow\uparrow\downarrow\rangle$	$+r_4e^{i\theta_4}$
$\|\downarrow\downarrow\uparrow\uparrow\downarrow\uparrow\rangle$	$-r_2e^{i\theta_2}$ $-r_4e^{i\theta_4}$
$\|\downarrow\downarrow\downarrow\uparrow\uparrow\uparrow\rangle$	$-r_5e^{i\theta_5}$
$\|\uparrow\uparrow\uparrow\downarrow\downarrow\downarrow\rangle$	$+r_5e^{i\theta_5}$
$\|\uparrow\uparrow\downarrow\uparrow\downarrow\downarrow\rangle$	$-r_2e^{i\theta_2}$ $-r_5e^{i\theta_5}$
$\|\downarrow\downarrow\uparrow\downarrow\uparrow\uparrow\rangle$	$+r_2e^{i\theta_2}$ $+r_5e^{i\theta_5}$
$\|\downarrow\uparrow\uparrow\uparrow\downarrow\downarrow\rangle$	$-r_3e^{i\theta_3}$
$\|\uparrow\downarrow\downarrow\downarrow\uparrow\uparrow\rangle$	$+r_3e^{i\theta_3}$
$\|\downarrow\uparrow\downarrow\downarrow\uparrow\uparrow\rangle$	$-r_2e^{i\theta_2}$ $-r_3e^{i\theta_3}$
$\|\uparrow\downarrow\uparrow\uparrow\downarrow\downarrow\rangle$	$+r_2e^{i\theta_2}$ $+r_3e^{i\theta_3}$

TABLE II: Basis states $|\psi_k^z\rangle$ of Eq. (10) for a six-qubit system and the corresponding coefficients $e^{i\delta_k}$ determined from the equation $|\Psi^6\rangle = |\Psi_6\rangle_{hom}$.

Six Qubit maximal E_v^2 states: The linearly independent states in this case are five in number (i.e., the five non-crossing Rumer diagrams of Fig. 3). Thus as in the four-qubit case, we begin with the following general linear superposition:

$$\begin{aligned}
|\Psi^6\rangle &= r_1e^{i\theta_1}\left[|\Phi_{12}^{S_{12}=0}\rangle \otimes |\Phi_{34}^{S_{34}=0}\rangle \otimes |\Phi_{56}^{S_{56}=0}\rangle\right] \\
&+ r_2e^{i\theta_2}\left[|\Phi_{61}^{S_{61}=0}\rangle \otimes |\Phi_{23}^{S_{23}=0}\rangle \otimes |\Phi_{45}^{S_{45}=0}\rangle\right] \\
&+ r_3e^{i\theta_3}\left[|\Phi_{12}^{S_{12}=0}\rangle \otimes |\Phi_{36}^{S_{36}=0}\rangle \otimes |\Phi_{45}^{S_{45}=0}\rangle\right] \\
&+ r_4e^{i\theta_4}\left[|\Phi_{23}^{S_{23}=0}\rangle \otimes |\Phi_{14}^{S_{14}=0}\rangle \otimes |\Phi_{56}^{S_{56}=0}\rangle\right] \\
&+ r_5e^{i\theta_5}\left[|\Phi_{16}^{S_{16}=0}\rangle \otimes |\Phi_{25}^{S_{25}=0}\rangle \otimes |\Phi_{34}^{S_{34}=0}\rangle\right], \qquad (15)
\end{aligned}$$

and find solutions that homogenize $|\Psi^6\rangle$, i.e., make $|\Psi^6\rangle$ assume the $|\Psi_6\rangle_{hom}$ form in Eq. (10). Next, we evaluate Eq. (15) and get the various coefficients for each basis state $|\psi_k^z\rangle$ mentioned in Eq. (10). The expressions for the coefficients $e^{i\delta_k}$ in Eq. (10) are shown in Table II. As in the four-qubit case, we make the state in Eq. (15) homogeneous, i.e., assume the form given in Eq. (10).

We observe that, since there are only five linearly independent Rumer states, we can construct at most five linearly independent superpositions of the form $|\Psi^6\rangle$ given by Eq. (15); thus we can expect five independent sets of coefficients $r_i e^{i\theta_i}$ producing homogeneity. Here, we present five linearly independent solutions:

1. $\{r_1 = r_2 = 0; (r_3 e^{i\theta_3}, r_4 e^{i\theta_4}, r_5 e^{i\theta_5}) = (\omega_4, \omega_4^2, \omega_4^3)\}$,
2. $\{r_1 = r_2 = 0; (r_3 e^{i\theta_3}, r_4 e^{i\theta_4}, r_5 e^{i\theta_5}) = (\omega_4^*, \omega_4^{*2}, \omega_4^{*3})\}$,
3. $\{r_1 = r_2 = 0; (r_3 e^{i\theta_3}, r_4 e^{i\theta_4}, r_5 e^{i\theta_5}) = (-1, +1, -1)\}$,
4. $\{r_1 e^{i\theta_1} = -1 + e^{i\alpha}; r_2 e^{i\theta_2} = 1 + e^{i\alpha};$ $(r_3 e^{i\theta_3}, r_4 e^{i\theta_4}, r_5 e^{i\theta_5}) = (-1, -1, -1)\}$,
5. $\{r_1 e^{i\theta_1} = -1 + e^{-i\alpha}; r_2 e^{i\theta_2} = 1 + e^{-i\alpha};$ $(r_3 e^{i\theta_3}, r_4 e^{i\theta_4}, r_5 e^{i\theta_5}) = (-1, -1, -1)\}$.

where $\omega_4 = e^{i2\pi/4}$ is a fourth root of unity and $e^{i\alpha}$ is a complex number. In arriving at the above solutions, use has been made of the fact that when $\sum_{j=1}^{4} e^{i\alpha_j} = 0$, we have two pairs of unit vectors with each pair giving a zero sum (as shown in Fig. 4 for one the three possibilities). The states corresponding to the first and the second solutions are

$$\begin{aligned}|\Psi_a^6\rangle \; = \; & \omega_4(|\Phi_{12}^{S_{12}=0}\rangle \otimes |\Phi_{36}^{S_{36}=0}\rangle \otimes |\Phi_{45}^{S_{45}=0}\rangle) \\ & +\omega_4^2(|\Phi_{23}^{S_{23}=0}\rangle \otimes |\Phi_{14}^{S_{14}=0}\rangle \otimes |\Phi_{56}^{S_{56}=0}\rangle) \\ & +\omega_4^3(|\Phi_{16}^{S_{16}=0}\rangle \otimes |\Phi_{25}^{S_{25}=0}\rangle \otimes |\Phi_{34}^{S_{34}=0}\rangle), \end{aligned} \tag{16}$$

and its complex conjugate, while the state that corresponds to the third solution is

$$\begin{aligned}|\Psi_b^6\rangle \; = \; & -(|\Phi_{12}^{S_{12}=0}\rangle \otimes |\Phi_{36}^{S_{36}=0}\rangle \otimes |\Phi_{45}^{S_{45}=0}\rangle) \\ & +(|\Phi_{23}^{S_{23}=0}\rangle \otimes |\Phi_{14}^{S_{14}=0}\rangle \otimes |\Phi_{56}^{S_{56}=0}\rangle) \\ & -(|\Phi_{16}^{S_{16}=0}\rangle \otimes |\Phi_{25}^{S_{25}=0}\rangle \otimes |\Phi_{34}^{S_{34}=0}\rangle). \end{aligned} \tag{17}$$

The states that are obtained from the fourth and the fifth solutions can be written as

$$\begin{aligned}|\Psi_c^6\rangle \; = \; & (-1 + e^{i\alpha}) \left[|\Phi_{12}^{S_{12}=0}\rangle \otimes |\Phi_{34}^{S_{34}=0}\rangle \otimes |\Phi_{56}^{S_{56}=0}\rangle\right] \\ & +(1 + e^{i\alpha}) \left[|\Phi_{61}^{S_{61}=0}\rangle \otimes |\Phi_{23}^{S_{23}=0}\rangle \otimes |\Phi_{45}^{S_{45}=0}\rangle\right] \\ & - \left[|\Phi_{12}^{S_{12}=0}\rangle \otimes |\Phi_{36}^{S_{36}=0}\rangle \otimes |\Phi_{45}^{S_{45}=0}\rangle\right] \\ & - \left[|\Phi_{23}^{S_{23}=0}\rangle \otimes |\Phi_{14}^{S_{14}=0}\rangle \otimes |\Phi_{56}^{S_{56}=0}\rangle\right] \\ & - \left[|\Phi_{16}^{S_{16}=0}\rangle \otimes |\Phi_{25}^{S_{25}=0}\rangle \otimes |\Phi_{34}^{S_{34}=0}\rangle\right]. \end{aligned} \tag{18}$$

and its complex conjugate. Using $e^{i\alpha} = -i (= -\omega_4)$, the state in Eq. (18) can be rewritten as

$$\begin{aligned}|\Psi_c^6\rangle \; = \; & \omega_4(|\Phi_{12}^{S_{12}=0}\rangle \otimes |\Phi_{34}^{S_{34}=0}\rangle \otimes |\Phi_{65}^{S_{65}=0}\rangle) \\ & +\omega_4^2(|\Phi_{14}^{S_{14}=0}\rangle \otimes |\Phi_{25}^{S_{25}=0}\rangle \otimes |\Phi_{36}^{S_{36}=0}\rangle) \\ & +\omega_4^3(|\Phi_{61}^{S_{61}=0}\rangle \otimes |\Phi_{23}^{S_{23}=0}\rangle \otimes |\Phi_{45}^{S_{45}=0}\rangle). \end{aligned} \tag{19}$$

This state represents the superposition of the three Rumer diagrams of Fig. 3(a) with the second term in the sum representing crossing singlets.

Evaluating the tensor products in the above Eqs. (16), (17), and (19), we rewrite these states as

$$\begin{aligned}|\Psi_a^6\rangle \; = \; & [(|\uparrow\downarrow\uparrow\downarrow\uparrow\downarrow\rangle - |\downarrow\uparrow\downarrow\uparrow\downarrow\uparrow\rangle) + \omega_4(|\uparrow\downarrow\uparrow\uparrow\downarrow\downarrow\rangle + |\uparrow\downarrow\downarrow\downarrow\uparrow\uparrow\rangle + |\downarrow\uparrow\uparrow\downarrow\uparrow\downarrow\rangle - |\uparrow\downarrow\downarrow\uparrow\downarrow\uparrow\rangle - |\downarrow\uparrow\uparrow\uparrow\downarrow\downarrow\rangle - |\downarrow\uparrow\downarrow\downarrow\uparrow\uparrow\rangle) \\ & + \omega_4^2(|\uparrow\uparrow\downarrow\downarrow\uparrow\downarrow\rangle + |\uparrow\downarrow\uparrow\downarrow\downarrow\uparrow\rangle + |\downarrow\downarrow\uparrow\uparrow\uparrow\downarrow\rangle - |\uparrow\uparrow\downarrow\downarrow\downarrow\uparrow\rangle - |\downarrow\uparrow\downarrow\uparrow\uparrow\downarrow\rangle - |\downarrow\downarrow\uparrow\uparrow\downarrow\uparrow\rangle) \\ & + \omega_4^3(|\uparrow\uparrow\uparrow\downarrow\downarrow\downarrow\rangle + |\downarrow\downarrow\uparrow\downarrow\uparrow\uparrow\rangle + |\uparrow\downarrow\downarrow\uparrow\uparrow\downarrow\rangle - |\uparrow\uparrow\downarrow\uparrow\downarrow\downarrow\rangle - |\downarrow\uparrow\uparrow\downarrow\downarrow\uparrow\rangle - |\downarrow\downarrow\downarrow\uparrow\uparrow\uparrow\rangle)], \end{aligned} \tag{20}$$

$$\begin{aligned}|\Psi_b^6\rangle \; = \; & [(|\uparrow\downarrow\uparrow\downarrow\uparrow\downarrow\rangle - |\downarrow\uparrow\downarrow\uparrow\downarrow\uparrow\rangle) - (|\uparrow\downarrow\uparrow\uparrow\downarrow\downarrow\rangle + |\uparrow\downarrow\downarrow\downarrow\uparrow\uparrow\rangle + |\downarrow\uparrow\uparrow\downarrow\uparrow\downarrow\rangle - |\uparrow\downarrow\downarrow\uparrow\downarrow\uparrow\rangle - |\downarrow\uparrow\uparrow\uparrow\downarrow\downarrow\rangle - |\downarrow\uparrow\downarrow\downarrow\uparrow\uparrow\rangle) \\ & + (|\uparrow\uparrow\downarrow\downarrow\uparrow\downarrow\rangle + |\uparrow\downarrow\uparrow\downarrow\downarrow\uparrow\rangle + |\downarrow\downarrow\uparrow\uparrow\uparrow\downarrow\rangle - |\uparrow\uparrow\downarrow\downarrow\downarrow\uparrow\rangle - |\downarrow\uparrow\downarrow\uparrow\uparrow\downarrow\rangle - |\downarrow\downarrow\uparrow\uparrow\downarrow\uparrow\rangle) \\ & - (|\uparrow\uparrow\uparrow\downarrow\downarrow\downarrow\rangle + |\downarrow\downarrow\uparrow\downarrow\uparrow\uparrow\rangle + |\uparrow\downarrow\downarrow\uparrow\uparrow\downarrow\rangle - |\uparrow\uparrow\downarrow\uparrow\downarrow\downarrow\rangle - |\downarrow\uparrow\uparrow\downarrow\downarrow\uparrow\rangle - |\downarrow\downarrow\downarrow\uparrow\uparrow\uparrow\rangle)], \end{aligned} \tag{21}$$

and

$$\begin{aligned}|\Psi_c^6\rangle \; = \; & [(|\uparrow\downarrow\uparrow\downarrow\uparrow\downarrow\rangle - |\downarrow\uparrow\downarrow\uparrow\downarrow\uparrow\rangle) + \omega_4(|\uparrow\downarrow\uparrow\downarrow\downarrow\uparrow\rangle + |\uparrow\downarrow\downarrow\uparrow\uparrow\downarrow\rangle + |\downarrow\uparrow\uparrow\downarrow\uparrow\downarrow\rangle - |\uparrow\downarrow\downarrow\uparrow\downarrow\uparrow\rangle - |\downarrow\uparrow\uparrow\downarrow\downarrow\uparrow\rangle - |\downarrow\uparrow\downarrow\uparrow\uparrow\downarrow\rangle) \\ & + \omega_4^2(|\uparrow\uparrow\uparrow\downarrow\downarrow\downarrow\rangle + |\uparrow\downarrow\downarrow\downarrow\uparrow\uparrow\rangle + |\downarrow\downarrow\uparrow\uparrow\uparrow\downarrow\rangle - |\uparrow\uparrow\downarrow\downarrow\downarrow\uparrow\rangle - |\downarrow\uparrow\uparrow\uparrow\downarrow\downarrow\rangle - |\downarrow\downarrow\downarrow\uparrow\uparrow\uparrow\rangle) \\ & + \omega_4^3(|\uparrow\uparrow\downarrow\downarrow\uparrow\downarrow\rangle + |\uparrow\downarrow\uparrow\uparrow\downarrow\downarrow\rangle + |\downarrow\downarrow\uparrow\downarrow\uparrow\uparrow\rangle - |\uparrow\uparrow\downarrow\uparrow\downarrow\downarrow\rangle - |\downarrow\uparrow\downarrow\downarrow\uparrow\uparrow\rangle - |\downarrow\downarrow\uparrow\uparrow\downarrow\uparrow\rangle)]. \end{aligned} \tag{22}$$

B. Producing isotropy in homogeneous states

Next, we produce isotropy in a given homogeneous state; such states should also yield the entanglement value $E_{v,max}^2$. The condition of isotropy in a homogeneous state can be expressed as $\sum_i S_i^\alpha|\Psi_N\rangle_{hom} = 0$ with $\alpha = x, y, z$; this implies that $\sum_i S_i^+|\Psi_N\rangle_{hom} = 0$. Now, reflection about z-axis for $\Phi_{ij}^{S_{ij}=0}$ produces $-\Phi_{ij}^{S_{ij}=0}$; then in an isotropic $S_T = 0$ state comprising of $\frac{N}{2}$ singlets, reflection leads to a coefficient of $(-1)^{\frac{N}{2}}$ for the parent state. Hence, in the homogeneous state of Eq. (10), imposing isotropy implies that flipping all spins should produce a coefficient of $(-1)^{\frac{N}{2}}$ for the parent state; in fact, the coefficients $e^{i\delta_k}$ of the basis state $|\sigma_1^z\sigma_2^z...\sigma_N^z\rangle$ and its spin flipped version differ only by a factor $(-1)^{\frac{N}{2}}$. Thus the number of unknown coefficients $e^{i\delta_k}$ in Eq. (10) is reduced to $0.5\left({}^N C_{\frac{N}{2}}\right)$; this also implies that $\sum_i S_i^-|\Psi_N\rangle_{hom} = 0$ yields the same equations as the condition $\sum_i S_i^+|\Psi_N\rangle_{hom} = 0$. Therefore, we can write the four-qubit homogeneous state as

$$\begin{aligned}|\Psi_4\rangle_{hom} &= e^{i\phi_1}[|\uparrow\downarrow\uparrow\downarrow\rangle + |\downarrow\uparrow\downarrow\uparrow\rangle] \\ &+ e^{i\phi_2}[|\uparrow\downarrow\downarrow\uparrow\rangle + |\downarrow\uparrow\uparrow\downarrow\rangle] \\ &+ e^{i\phi_3}[|\uparrow\uparrow\downarrow\downarrow\rangle + |\downarrow\downarrow\uparrow\uparrow\rangle]. \qquad (23)\end{aligned}$$

Furthermore, the condition of isotropy in the above four-qubit homogeneous state yields

$$\begin{aligned}\sum_{i=1}^{4} S_i^+|\Psi_4\rangle_{hom} &= (e^{i\phi_1} + e^{i\phi_2} + e^{i\phi_3})\,[|\uparrow\uparrow\uparrow\downarrow\rangle + |\uparrow\downarrow\uparrow\uparrow\rangle \\ &\qquad |\uparrow\uparrow\downarrow\uparrow\rangle + |\downarrow\uparrow\uparrow\uparrow\rangle] \\ &= 0. \qquad (24)\end{aligned}$$

This leads to the expression $e^{i\phi_1} + e^{i\phi_2} + e^{i\phi_3} = 0$, i.e., zero valued coefficients for all the four basis states. The only two possible solutions to this equation (up to a phase factor) are $\{e^{i\phi_1} = 1, e^{i\phi_2} = \omega_3, e^{i\phi_3} = \omega_3^2\}$ and its complex conjugate. The states obtained from these solutions are the same as those obtained earlier by imposing homogeneity on isotropic states and represent the four-qubit HS-state and its complex conjugate.

Next, we consider the case of six-qubit homogeneous state which can be written as:

$$\begin{aligned}|\Psi_6\rangle_{hom} = \quad & e^{i\phi_1}\,[|\uparrow\downarrow\uparrow\downarrow\uparrow\downarrow\rangle - |\downarrow\uparrow\downarrow\uparrow\downarrow\uparrow\rangle] \\ + \; & e^{i\phi_2}\,[|\downarrow\uparrow\uparrow\downarrow\uparrow\downarrow\rangle - |\uparrow\downarrow\downarrow\uparrow\downarrow\uparrow\rangle] \\ + \; & e^{i\phi_3}\,[|\uparrow\downarrow\downarrow\uparrow\uparrow\downarrow\rangle - |\downarrow\uparrow\uparrow\downarrow\downarrow\uparrow\rangle] \\ + \; & e^{i\phi_4}\,[|\downarrow\uparrow\downarrow\uparrow\uparrow\downarrow\rangle - |\uparrow\downarrow\uparrow\downarrow\downarrow\uparrow\rangle] \\ + \; & e^{i\phi_5}\,[|\uparrow\uparrow\downarrow\downarrow\uparrow\downarrow\rangle - |\downarrow\downarrow\uparrow\uparrow\downarrow\uparrow\rangle] \\ + \; & e^{i\phi_6}\,[|\uparrow\uparrow\downarrow\downarrow\downarrow\uparrow\rangle - |\downarrow\downarrow\uparrow\uparrow\uparrow\downarrow\rangle] \\ + \; & e^{i\phi_7}\,[|\downarrow\downarrow\downarrow\uparrow\uparrow\uparrow\rangle - |\uparrow\uparrow\uparrow\downarrow\downarrow\downarrow\rangle] \\ + \; & e^{i\phi_8}\,[|\uparrow\uparrow\downarrow\uparrow\downarrow\downarrow\rangle - |\downarrow\downarrow\uparrow\downarrow\uparrow\uparrow\rangle] \\ + \; & e^{i\phi_9}\,[|\downarrow\uparrow\uparrow\uparrow\downarrow\downarrow\rangle - |\uparrow\downarrow\downarrow\downarrow\uparrow\uparrow\rangle] \\ + \; & e^{i\phi_{10}}\,[|\downarrow\uparrow\downarrow\downarrow\uparrow\uparrow\rangle - |\uparrow\downarrow\uparrow\uparrow\downarrow\downarrow\rangle]. \qquad (25)\end{aligned}$$

Basis states contained in $\sum_{i=1}^{6} S_i^+ \mid \Psi^6\rangle_{hom}$.	Zero valued coefficients of basis states obtained from using isotropy on $\mid \Psi_6\rangle_{hom}$.
$\lvert\uparrow\uparrow\uparrow\downarrow\uparrow\downarrow\rangle$	$e^{i\phi_1} + e^{i\phi_2} + e^{i\phi_5} - e^{i\phi_7}$
$\lvert\uparrow\downarrow\uparrow\uparrow\uparrow\downarrow\rangle$	$e^{i\phi_1} + e^{i\phi_3} - e^{i\phi_6} - e^{i\phi_{10}}$
$\lvert\uparrow\downarrow\uparrow\downarrow\uparrow\uparrow\rangle$	$e^{i\phi_1} - e^{i\phi_4} - e^{i\phi_8} - e^{i\phi_9}$
$\lvert\downarrow\uparrow\uparrow\uparrow\uparrow\downarrow\rangle$	$e^{i\phi_2} + e^{i\phi_4} + e^{i\phi_9} - e^{i\phi_6}$
$\lvert\downarrow\uparrow\uparrow\downarrow\uparrow\uparrow\rangle$	$e^{i\phi_2} - e^{i\phi_3} - e^{i\phi_8} + e^{i\phi_{10}}$
$\lvert\uparrow\uparrow\downarrow\uparrow\uparrow\downarrow\rangle$	$e^{i\phi_3} + e^{i\phi_4} + e^{i\phi_5} + e^{i\phi_8}$
$\lvert\downarrow\uparrow\downarrow\uparrow\uparrow\uparrow\rangle$	$-e^{i\phi_1} + e^{i\phi_4} + e^{i\phi_7} + e^{i\phi_{10}}$
$\lvert\uparrow\uparrow\downarrow\downarrow\uparrow\uparrow\rangle$	$e^{i\phi_5} + e^{i\phi_6} - e^{i\phi_9} + e^{i\phi_{10}}$
$\lvert\uparrow\uparrow\uparrow\downarrow\downarrow\uparrow\rangle$	$-e^{i\phi_3} - e^{i\phi_4} + e^{i\phi_6} - e^{i\phi_7}$
$\lvert\uparrow\uparrow\downarrow\uparrow\downarrow\uparrow\rangle$	$-e^{i\phi_1} - e^{i\phi_2} + e^{i\phi_6} + e^{i\phi_8}$
$\lvert\uparrow\downarrow\downarrow\uparrow\uparrow\uparrow\rangle$	$-e^{i\phi_2} + e^{i\phi_3} + e^{i\phi_7} - e^{i\phi_9}$
$\lvert\downarrow\downarrow\uparrow\uparrow\uparrow\uparrow\rangle$	$-e^{i\phi_5} - e^{i\phi_6} + e^{i\phi_7} - e^{i\phi_8}$
$\lvert\uparrow\uparrow\uparrow\uparrow\downarrow\downarrow\rangle$	$-e^{i\phi_7} + e^{i\phi_8} + e^{i\phi_9} - e^{i\phi_{10}}$
$\lvert\downarrow\uparrow\uparrow\uparrow\downarrow\uparrow\rangle$	$-e^{i\phi_1} - e^{i\phi_3} - e^{i\phi_5} + e^{i\phi_9}$
$\lvert\uparrow\downarrow\uparrow\uparrow\downarrow\uparrow\rangle$	$-e^{i\phi_2} - e^{i\phi_4} - e^{i\phi_5} - e^{i\phi_{10}}$

TABLE III: The basis states and the corresponding zero valued coefficients obtained from the condition of isotropy $\sum_{i=1}^{6} S_i^+|\Psi_6\rangle_{hom} = 0$.

The isotropy condition for the above six-qubit homogeneous state (expressed as $\sum_{i=1}^{6} S_i^+|\Psi_N\rangle_{hom} = 0$) yields the various basis states and the corresponding coefficients shown in table III. The set of fifteen equations (corresponding to the zero valued coefficients of the basis states) in table III can be reduced to the following set of five linearly independent equations:

$$e^{i\phi_1} + e^{i\phi_2} + e^{i\phi_5} - e^{i\phi_7} = 0 \qquad (26)$$

$$e^{i\phi_1} + e^{i\phi_3} - e^{i\phi_6} - e^{i\phi_{10}} = 0 \qquad (27)$$

$$e^{i\phi_1} - e^{i\phi_4} - e^{i\phi_8} - e^{i\phi_9} = 0 \qquad (28)$$

$$e^{i\phi_1} - e^{i\phi_4} - e^{i\phi_7} - e^{i\phi_{10}} = 0 \qquad (29)$$

$$e^{i\phi_1} + e^{i\phi_2} - e^{i\phi_6} - e^{i\phi_8} = 0. \qquad (30)$$

The above equations can be viewed as the sum of unit vectors on a circle in the complex plane. Since the sum is of the form $\sum_{j=1}^{4} e^{i\alpha_j} = 0$, it implies the conditions shown in Fig. 4. The five linearly independent solutions of the above set of Eqs. (26)-(30) are given in Table IV. This set of solutions produces the same entangled states $[|\Psi_a^6\rangle$, $(|\Psi_a^6\rangle)^*$, $|\Psi_b^6\rangle$, $|\Psi_c^6\rangle$, and $(|\Psi_c^6\rangle)^*]$ as obtained in the previous section.

C. Discussion and comparison

We will now discuss generating $E^2_{v,max}$ RVB states for the general case of an even N spin system. The number of coefficients $r_i e^{i\theta_i}$, needed to generate a superposed state $|\Psi^N\rangle$ using all non-crossing Rumer states,

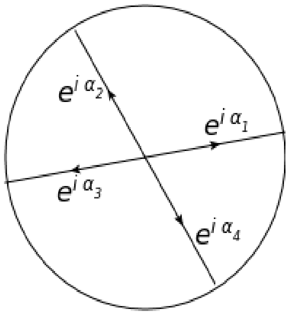

FIG. 4: Geometric depiction of zero sum of four unit vectors on a unit circle in the complex plane. This represents one of the three possibilities of the zero sum $\sum_{j=1}^{4} e^{i\alpha_j} = 0$. The other two possibilities are $e^{i\alpha_1} + e^{i\alpha_2} = 0$, $e^{i\alpha_3} + e^{i\alpha_4} = 0$; and $e^{i\alpha_1} + e^{i\alpha_4} = 0$, $e^{i\alpha_2} + e^{i\alpha_3} = 0$.

is the same as the total number of linearly independent Rumer states ${}^N C_{\frac{N}{2}} - {}^N C_{\frac{N}{2}-1}$. The number of independent basis states $|\psi_k^z\rangle$ in Eq. (10) is $0.5 \left({}^N C_{\frac{N}{2}}\right)$. On setting $|\Psi^N\rangle = |\Psi_N\rangle_{hom}$ and equating the coefficients of the various basis states, we get $0.5 \left({}^N C_{\frac{N}{2}}\right)$ equations; from these equations, on eliminating $r_i e^{i\theta_i}$ in terms of the various $e^{i\delta_k}$, we get $-0.5 \left({}^N C_{\frac{N}{2}}\right) + {}^N C_{\frac{N}{2}-1}$ number of linearly independent equations [of the form of Eqs. (26)-(30) when $N = 6$] in terms of $0.5 \left({}^N C_{\frac{N}{2}}\right)$ number of unknown coefficients $e^{i\delta_k}$. Thus, we expect the number of independent $E_{v,max}^2$ RVB states to be equal to ${}^N C_{\frac{N}{2}} - {}^N C_{\frac{N}{2}-1}$ (i.e., the number of unknown $e^{i\delta_k}$ minus the number of independent equations) which is the same as the number of linearly independent Rumer states. For instance, for $N = 8$, we get 21 linearly independent equations in terms of 35 different $e^{i\delta_k}$; thus the number of independent $E_{v,max}^2$ RVB states is 14 ($= 35 - 21$) which is the total number of non-crossing Rumer states.

Coefficients in	Five linearly independent solutions				
Eqs. (26)-(30)	Sol. 1	Sol. 2	Sol. 3	Sol. 4	Sol. 5
$e^{i\phi_1}$	1	1	1	1	1
$e^{i\phi_2}$	ω_4	ω_4^*	-1	$-e^{i\alpha}$	$-e^{-i\alpha}$
$e^{i\phi_3}$	ω_4^3	ω_4^{*3}	-1	$-e^{i\alpha}$	$-e^{-i\alpha}$
$e^{i\phi_4}$	$-\omega_4^2$	$-\omega_4^{*2}$	-1	$e^{i\alpha}$	$e^{-i\alpha}$
$e^{i\phi_5}$	ω_4^2	ω_4^{*2}	1	$e^{i\alpha}$	$e^{-i\alpha}$
$e^{i\phi_6}$	$-\omega_4^2$	$-\omega_4^{*2}$	-1	1	1
$e^{i\phi_7}$	$-\omega_4^3$	$-\omega_4^{*3}$	1	1	1
$e^{i\phi_8}$	$-\omega_4^3$	$-\omega_4^{*3}$	1	$-e^{i\alpha}$	$-e^{-i\alpha}$
$e^{i\phi_9}$	$-\omega_4$	$-\omega_4^*$	1	1	1
$e^{i\phi_{10}}$	$-\omega_4$	$-\omega_4^*$	1	$-e^{i\alpha}$	$-e^{-i\alpha}$

TABLE IV: Sets of five linearly independent solutions of the Eqs. (26)-(30).

Next, we observe that the von Neumann entropy E_v^2, for two-qubit reduced density matrix obtained from $|\Psi_a^6\rangle$, $(|\Psi_a^6\rangle)^*$, $|\Psi_b^6\rangle$, $|\Psi_c^6\rangle$, or $(|\Psi_c^6\rangle)^*$, is 1.921964 which is the same as $E_{v,max}^2$ proposed by our general formula in Eq. (8). The conjecture made by Brown *et al.* [13] that the multi-qubit maximally entangled states always have their reduced single qubit density matrix maximally mixed is satisfied by our states $|\Psi^6\rangle$. It should be noted that the highly entangled six-qubit state reported in Ref. [10], although yields a higher entanglement, is not an eigenstate of the S_{Total}^z operator.

Cabello [37] has also constructed supersinglets of four and six qubits which are decoherence free. However, the average two particle von Neumann entanglement entropy E_v^2 for these supersinglets is less than the entanglement for our states constructed above. In the case of the four qubit supersinglet state $\left|\mathcal{S}_4^{(2)}\right\rangle$, the entanglement entropies for all possible bipartitions are given by $E_v(\rho_{12}) = E_v(\rho_{34}) = 1.5849$, $E_v(\rho_{13}) = E_v(\rho_{24}) = 1.2075$, $E_v(\rho_{14}) = E_v(\rho_{23}) = 1.2075$ which together yield the average two particle entropy value 1.3333, i.e., a quantity clearly smaller than the von Neumann entropy $E_v^2 = 1 + 0.5 \log_2 3 \approx 1.79248$ obtained for the four-qubit maximally entangled HS state. In the six qubit supersinglet $\left|\mathcal{S}_6^{(2)}\right\rangle$ case, the various bipartitions produce the average entropy $E_v^2 = 1.657996$ which is noticeably smaller than the entropy value $E_{v,max}^2 = 1.921964$ obtained for our six qubit entangled states.

IV. GENERATING HIGHLY ENTANGLED GROUND STATES USING IIRHM

In this section we will demonstrate that the $E_{v,max}^2$ entangled states obtained in the previous section from the homogenization of isotropic states (or from imposing isotropy on homogeneous states) are the ground states of a spin Hamiltonian. Thus we begin with the IIRHM Hamiltonian

$$H_{\mathrm{IIRHM}} = J \sum_{i,j>i} \vec{S}_i . \vec{S}_j = \frac{J}{2} \left[\left(\sum_i \vec{S}_i \right)^2 - \left(\sum_i \vec{S}_i^{\,2} \right) \right], \quad (31)$$

and show that certain superpositions of the ground states of IIRHM will produce the same amount of entanglement as given by Eq. (8). We observe that $[S_{Total}^z, H_{\mathrm{IIRHM}}] = 0$ and $[S_{Total}^2, H_{\mathrm{IIRHM}}] = 0$. In Eq. (31), we take $J = J^\star/(N-1)$ (where $J^\star$ is a finite quantity) so that the energy per site remains finite as $N \to \infty$. The eigenstates of $H_{\rm IIRHM}$ correspond to eigenenergies

$$E_{S_T} = \frac{J}{2}\left[S_T(S_T+1) - \frac{3N}{4}\right], \qquad (32)$$

where S_T is the total spin eigenvalue. The ground state corresponds to $S_T = 0$ which is rotationally invariant and also implies that $S_T^z = 0$. Next, we note the interesting fact that

$$[\vec{S_1}.\vec{S_3} + \vec{S_2}.\vec{S_4} + \vec{S_1}.\vec{S_4} + \vec{S_2}.\vec{S_3}]|\Phi_{12}^{S_{12}=0}\rangle \otimes |\Phi_{34}^{S_{34}=0}\rangle = 0,$$

using which it can be shown that any $S_T = 0$ state made up of $N/2$ singlets will be an eigenstate of Eq. (31). Thus the Rumer states are ground states of $H_{\rm IIRHM}$. Hence, for a homogenized linear combination of non-crossing Rumer states, the entanglement is given by Eq. (8).

It is important to note that, while all possible $S_T = 0$ states are ground states of IIRHM, for some Hamiltonians only some of the possible $S_T = 0$ states are ground states. For instance, for the nearest-neighbor antiferromagnetic Heisenberg Hamiltonian or for the Majumdar-Ghosh model Hamiltonian [38] only some of the possible $S_T = 0$ states are ground states and consequently (for these systems) it is not possible to construct a homogenized linear combination of $S_T = 0$ ground states that produces maximal possible entanglement $E^2_{v,max}$ given by Eq. (8).

V. RESONATING-VALENCE-BOND PICTURE

The construction of our entangled maximal E_v^2 states that form the ground states of IIRHM can be visualized by using a RVB picture. Our maximal E_v^2 states can be regarded as a new class of RVB states made of homogenized superposition of isotropic $S_T = 0$ valence bond states. We will now compare the entanglement properties of our RVB states and the general RVB states $|\Psi\rangle_{\rm rvb}$ of Ref. 30 given below:

$$|\Psi\rangle_{\rm rvb} = \sum_{\substack{i_\alpha \in A \\ j_\beta \in B}} f(i_1, ..., i_M, j_1, ..., j_M)|(i_1, j_1)...(i_M, j_M)\rangle,$$

where M represents the number of sites in each sub-lattice and f is assumed to be isotropic over the lattice. Also, $|(i_k, j_k)\rangle \equiv \frac{1}{\sqrt{2}}(|\uparrow\rangle_{i_k}|\downarrow\rangle_{j_k} - |\downarrow\rangle_{i_k}|\uparrow\rangle_{j_k})$ denotes the singlet dimer connecting a site in sub-lattice A with a site in sub-lattice B. The valence bond basis (used for the above RVB state $|\Psi\rangle_{\rm rvb}$) form an over complete set while our RVB states are constructed from a complete set of ${}^N C_{\frac{N}{2}} - {}^N C_{\frac{N}{2}-1}$ states.

The rotational invariance of the two qubit reduced density matrix of the RVB states allows us to write them in the form of a Werner state:

$$\rho_w(p) = p|(ij)\rangle\langle(ij)| + \frac{1-p}{4}I_4, \qquad (33)$$

where for $1/3 < p \leq 1$ the Werner state has the spins at i and j entangled with each other. For the special case of the "RVB gas" for the $|\Psi\rangle_{\rm rvb}$ state, where f is a constant (corresponding to equal amplitude superposition of all bipartite valence bond coverings), one gets the exact result $p = 1/3 + 2/(3N)$ which implies that all finite size systems have a non-zero tangle (or entanglement) between the two sites [30]. Next, for the "RVB liquid" case (involving equal amplitude superposition of all nearest-neighbor singlet valence bond coverings of a lattice), Monte Carlo calculations extrapolated to the thermodynamic limit yield $p = 0.3946(3) > 1/3$ [30], i.e., a non-zero tangle between the two sites [39]. In contrast, our maximal E_v^2 RVB states yield zero entanglement between the two spins for all system sizes as demonstrated below. It has been shown that the $SU(2)$ symmetry of the RVB states ensures that the two-spin correlation function and the parameter p of the Werner state are related as

$$\langle\Psi|\vec{S_i}.\vec{S_j}|\Psi\rangle = -\frac{3}{4}p. \qquad (34)$$

Then, since our RVB states produce

$$\langle S_i^x S_j^x\rangle = \langle S_i^y S_j^y\rangle = \langle S_i^z S_j^z\rangle = \frac{-1}{4(N-1)}, \qquad (35)$$

it follows that $p = \frac{1}{N-1}$ and thus for all even $N \geq 4$ systems we get zero entanglement between the two sites. Lastly, based on Ref. 30, we find that the monogamy argument yields the bound $p \leq 1/3 + 2/(3\sqrt{N-1})$ while the quantum telecloning argument produces the bound $p \leq 1/3 + 2/[3(N-1)]$. Compared to our exact value of $p = 1/(N-1)$, both these bounds are weaker bounds (i.e., show zero two-site entanglement with certainty only in the thermodynamic limit). Thus (among various RVB states) we see that our entangled high E_v^2 RVB states, while producing maximum entanglement between a pair and the rest of the system, yield zero entanglement among the two spins of the pair.

We will now remark on the entanglement of any set of n (> 2) sites with the rest of the system. The valence bond entanglement entropy picture, developed in references [31] and [32], uses the number of valence bond two-spin singlets shared by the two subsystems as a measure of their entanglement with each other. Thus, our 'homogenized' RVB states, will always have shared bonds between the two subsystems and thus show high bipartite entanglement. However, exact quantitative analysis needs to be carried out. Extending our approach to deriving the n-qubit reduced density matrix in terms of n-particle correlation functions (when $n > 2$) and obtaining entanglement expressions and wavefunctions corresponding to maximal bipartite entanglement is a non-trivial exercise and is left for future studies. In this connection, our notion of homogeneity [as expressed in Eq. (10)] is useful even for higher order correlation functions (since $|\Psi_N\rangle_{hom}$ generates correlation functions $\langle S_i^z S_j^z ... S_l^z S_m^z\rangle$ that are independent of the site indices $i, j, ..., l, m$ when no two site indices respresent the same site).

VI. CONCLUSIONS.

Although both spins in a two-spin singlet state $|\uparrow\downarrow\rangle - |\downarrow\uparrow\rangle$ are monogamous (i.e., they cannot be entangled with any other spin), by using a homogenized superposition of valence bond states (each of which is a product of $N/2$ two-spin singlets), we managed to distribute entanglement efficiently such that any pair is maximally entangled with the rest of the RVB system while concomitantly the constituent spins of the pair are completely unentangled with each other. Thus we get the converse of monogamy for a pair of spins! Now, while total spin zero states are quite commonly ground states (as shown by Lieb-Mattis theorem [40]), it has not been recognized that one can generate high bipartite E_v^2 entanglement from such states. Our maximal E_v^2 RVB states are physically realizable in systems such as infinite-range large U/t Hubbard model and infinite-range hard-core boson model with frustrated hopping [41] when they are at half-filling.

It can be shown that the eigenstates of our Hamiltonian IIRHM are decoherence free when the system is coupled to a bath of either local optical phonons or global optical phonons [42]. Since our RVB states (that are constructed from homogenization of VB states) form the ground states of IIRHM, they are decoherence free.

In summary, our maximal E_v^2 RVB states have led us to IIRHM for their realization and IIRHM in turn generated maximal E_v^2 states as highly robust ground states.

VII. ACKNOWLEDGMENTS

One of the authors (S. Y.) would like to thank G. Baskaran, R. Simon, and S. Ghosh for valuable discussions.

[1] M. A. Nielsen and I. Chuang, *Quantum Computation and Quantum Communication* (Cambridge University Press, Cambridge, 2000).

[2] G. Vidal, Phys. Rev. Lett. **91**, 147902 (2003).

[3] J. I. Latorre and A. Riera, J. Phys. A: Math. Theor. **42**, 504002 (2009).

[4] R. Horodecki, P. Horodecki, M. Horodecki, and K. Horodecki, Rev. Mod. Phys. **81**, 865 (2009).

[5] M. B. Plenio and S. Virmani, Quant. Inf. Comp. **7**, 1 (2007).

[6] D. A. Meyer and N. R. Wallach J. Math. Phys, **43** , 4273 (2002).

[7] A. J. Scott Phys. Rev. A **69**, 052330 (2004).

[8] A. R. R. Carvalho, F. Mintert, and A. Buchleitner, Phys. Rev. Lett, **93**, 230501 (2004).

[9] P. Facchi, G. Florio, and S. Pascazio, Phys. Rev. A **74**, 042331 (2006).

[10] A. Borras, A. R. Plastino, J. Batle, C. Zander, M. Casas, and A. Plastino, J. Phys. A: Math. Theor. **40**, 13407 (2007).

[11] G. Adesso and F. Illuminati, Phys. Rev. Lett, **99**, 150501 (2007).

[12] P. Facchi, G. Florio, G. Parisi, and S. Pascazio, Phys. Rev. A **77**, 060304(R) (2008).

[13] I. D. K. Brown, S. Stepney, A. Sudbery, and S. L. Braunstien, J. Phys. A: Math. Gen. **38**, 1119 (2005).

[14] A. Higuchi and A. Sudbery, Phys. Lett. A **273**, 213 (2000).

[15] B. Rothlisberger, J. Lehmann, D. S. Saraga, P. Traber, and D. Loss, Phys. Rev. Lett. **100**, 100502 (2008).

[16] P. Facchi, G. Florio, S. Pascazio, and F. Pepe, Phys. Rev. A **82**, 042313 (2010).

[17] F. Verstraete and J. I. Cirac, Phys. Rev. A **70**, 060302(R) (2004).

[18] Leong Chuan Kwek, Zhaohui Wei, Bei Zeng, e-print arXiv:1111.5084.

[19] S. Liang, B. Doucot, and P. W. Anderson, Phys. Rev. Lett. **61**, 365 (1988).

[20] M. Kohmoto, Phys. Rev. B **37**, 3812 (1988).

[21] Jie Lou and Anders W. Sandvik, Phys. Rev. B **76**, 104432 (2007).

[22] P. Fazekas and P. W. Anderson, Philos. Mag. **30**, 23 (1974).

[23] P. W. Anderson, Science **235**, 1196 (1987).

[24] P. W. Anderson, G. Baskaran, Z. Zou, and T. Hsu, Phys. Rev. Lett. **58**, 2790 (1987).

[25] P. A. Lee, N. Nagaosa, and X.-G. Wen, Rev. Mod. Phys. **78**, 17 (2006).

[26] T. Ishiguro, K. Yamaji, and G. Saito, Organic Superconductors (Springer, New York, 1998).

[27] E. A. Ekimov, V. A. Sidorov, E. D. Bauer, N. N. Mel'nik, N. J. Curro, J. D. Thompson, and S. M. Stishov, Nature (London) **428**, 542 (2004).

[28] A. Y. Kitaev, Ann. Phys. (N.Y.) **303**, 2 (2003).

[29] S. Liang and P. W. Anderson, Phy. Rev. Lett. **61**, 365 (1998)

[30] A. Chandran, D. Kaszilkowski, A. Sen(De), U. Sen and V. Vedral, Phys. Rev. Lett.**99**, 170502 (2007); D. Kaszlikowski, Aditi Sen(De), Ujjwal Sen, and V. Vedral, Phys. Rev. Lett. **101**, 248902 (2008); F. Alet, D.Braun, and G. Misguich, Phy.Rev.Lett. **101**, 248901 (2008).

[31] F. Alet, S. Capponi, N. Laflorencie, and M. Mambrini, Phys. Rev. Lett. **99**, 117204 (2007).

[32] R. W. Chhajlany, P. Tomczak and A. Wójcik, Phys. Rev. Lett. **99**, 167204 (2007)

[33] U. Glaser, H. Büttner, and H. Fehske, Phys. Rev. A. **68**, 032318 (2003).

[34] P. Rungta, V. Bužek, Carlton M. Caves, M. Hillery, and G. J. Milburn, Phys. Rev. A **64**, 042315 (2001).

[35] G. Rumer, Nachr. d. Ges. d. Wiss. zu Gottingen, M. P. Klasse, 337 (1932).

[36] L. Pauling, J. Chem. Phys. **1**, 280 (1933).

[37] A.Cabello, J. Mod. Opt. **50**, 10049 (2003).

[38] Chanchal K. Majumdar and Dipan K. Ghosh, J. Math. Phys. **10**, 1388 (1969).

[39] In Ref. 30 it was pointed out that the "RVB liquid" on a 4×4 square lattice gives $p > 1/3$ for periodic boundary conditions while it yields $p < 1/3$ in the interior of a

sample with open boundary conditions.

[40] E. Lieb and D. Mattis, Phys. Rev. **125**, 164 (1962).

[41] For examples of frustrated hopping, see F. Wang, F. Pollmann, and A. Vishwanath, Phys. Rev. Lett. **102**, 017203 (2009).

[42] M. Q. Lone, A. Dey and S. Yarlagadda, e-print arXiv:1205.4093.